Sigma J Eng Nat Sci, Vol. 39, No. 5, Supp 22, ICOMAA 2021, pp. 64–73, December, 2021

Sigma Journal of Engineering and Natural Sciences
Web page info: https://sigma.yildiz.edu.tr
DOI: 10.14744/sigma.2021.00043

Technical Note

Error analysis of an extended discontinuous galerkin method for highly-oscillatory problems

Donald FRENCH[1], Benjamin VAUGHAN[1], Şuayip TOPRAKSEVEN[2,*]

[1]Department of Mathematical Sciences, University of Cincinnati, Cincinnati, OH, USA
[2]Faculty of Engineering, Department of Computer Science, Artvin Çoruh University, Artvin, Turkey

ARTICLE INFO

Article history
Received: 22 October 2021
Accepted: 22 November 2021

Key words:
Discontinuous Galerkin, extended discontinuous Galerkin, high frequencies, elliptic boundary value problem
2010 MSC: Primary:
65N12; 65N15; 65N301

ABSTRACT

In this report we introduce an extended discontinuous Galerkin (XDG) method. Our XDG scheme is based on the Babuska-Zlamal approach and we apply it to a class of prototype elliptic boundary value problems that have solutions consisting of smooth functions perturbed by a set of high frequency modes which occupy a narrow band. The XDG scheme we study is enriched by trigonometric functions that cover the range of these perturbations. A theoretical error analysis is provided that shows the method converges and gives specifics on its accuracy. Computations with the XDG scheme further demonstrate the efficacy of this approach.

Cite this article as: Donald F, Benjamin V, Şuayip T. Error analysis of an extended discontinuous galerkin method for highly-oscillatory problems. Sigma J Eng Nat Sci 2021;39(Supp 22):64–73.

INTRODUCTION

A challenging problem when computing the numerical solution of ordinary and partial differential equations is dealing with systems that exhibit highly oscillatory behaviors. Highly oscillatory systems have solutions that exhibit a combination of a fast solution that oscillates quickly around a much more slowly varying solution. These systems can arise in many applications from molecular dynamics and bridging scale method for nanotubes [1, 2], high intesity focused ultrasound for cancer remidiation [3], electrical circuits [4], and quantum mechanics [5] among others. Due to their fast solution component, standard numerical approaches can require a large number of spatial and/or temporal steps in their discretization to accurately capture the high-frequency behavior.

Number of classical problems that exhibit high frequency, oscillatory solutions. The linear and nonlinear wave equations, Helmholtz equation, and Mathieu's equation are some examples. The study of the solution of these equations numerically when they exhibit high frequency oscillations requires significant computational effort or specialized numerical methods that capture the oscillations efficiently. For example, finite element methods can resolve

***Corresponding author.**
*E-mail address: topraksp@artvin.edu.tr

This paper was recommended for publication in revised form by Regional Editor Yusuf Zeren

the slowly varying component of the solution in space with a course to moderately refined mesh but will require a highly refined mesh to even resolve the high frequency components [6, 7]. It is often suggested it use a grid with at least ten mesh elements per wavelength. This can greatly increase the computational costs and restrict the ability to obtain a numerical approximation to small domains and short time intervals.

To reduce the computational complexity, various methods have been introduced to capture the highly oscillatory behavior without requiring a highly refined grid. For a review of finite element methods for time-harmonic acoustics, see [8].

One approach is to use known solutions of the given problem to extend or enrich the function space used to approximate the solution. The partition of unity method (PUM or PUFEM) is one such approach where plane wave solutions are added to the local finite element basis to approximate the solution to the Helmholtz equation [9]. A disadvantage of PUMs is ill-contintioning that can occur due to the choice of the approximation basis.

An alternative approach is least-squares methods [10] such as the ultraweak variational formulation (UWVF) [11, 12, 13, 14] where plane waves are used as a local, discontinuous basis for each element to approximate the solution to the Helmholtz equation. The approximate solution is generated by minimizing the least-squares difference of the solution and its normal derivative is minimized across element edges. In this approach, calculations are only performed on the element edges since the plane wave solutions satisfy the Helmholtz equation by construction. This approach requires a solution to the governing equation within each element, which could be difficult to obtain for more complex equations, and can exhibit ill-conditioning of the system matrix.

The discontinuous enrichment method (DEM), a standard finite element basis is used with additional discontinuous "enrichments" introduced to the approximation space. These enrichments contain the solution to the differential equation within the element and are discontinuous across the element boundaries. The continuity of the enrichments across the element boundaries are enforced weakly using Lagrange multipliers. As with the UWVF, the solution to the governing equation is required for each element. A comparison between PUFEM and UWVF is given by [15] and between PUFEM, DEM, and UWVF are given by [16].

The approach discussed in this paper uses a combination of the extended finite element method (XFEM) and the discontinuous Galerkin (dG) method [17, 18, 19]. The XFEM approach is based on the PUFEM and the generalized finite element method (GFEM) [20, 21] and was first developed in [22, 23] for the study of crack propagation. The GFEM combines the classical FEM with the PUFEM by retaining the mesh based nature of the FEM and was first applied to elliptic problems with voids [24, 25] and the Helmholtz equation [26, 27]. The XFEM strategy is to "enrich" a standard polynomial approximation space with non-smooth functions that approximate the solution in a way that is independent of the mesh. These "enrichment functions" add specialized shape function such as functions with jumps, large gradients, high-frequency oscillations, or singularities to the approximation space. These enrichment functions are included in addition to the classical polynomial basis. The enrichments can be either local or global in nature. The XFEM was initially developed for crack propagation in fracture mechanics but since has been used to study various problems such as Stefan problems [28], biofilm growth [29], and two-phase and free-surface flows [30]. For various reviews of the XFEM, see [32]. Recently, the proposed method has been applied to linear hyperbolic problem in [33].

A limitation of the XFEM is the often loss of the optimal convergence compared to the classical FEM. The suboptimal convergence can arise from elements where some but not all nodes are enriched. It was shown that these elements, called blending elements, have parasitic terms that limit the accuracy of the XFEM [33]. The effect of these terms has been reduced or eliminated using various methods such as applying an assumed strain method in the blending elements [34] or using higher-order spectral elements [35]. An alternative approach is to use a dG approach instead of the classical continuous FEM approach as the basis for the XFEM [36]. This approach uses an polynomial approximation space that is discontinuous across element boundaries. The makes both global and local enrichments local to each element, eliminating the effects of the blending elements. Continuity across element boundaries were enforced using a penalty method. This stability and convergence proofs of this approach for fracture mechanics was given in [37].

In this paper, we analyze an extended discontinuous Galerkin (XdG) method with high-frequency enrichments for oscillatory problems similar to the the enriched space-time discontinuous Galerkin methods for coupled atomistic/continuum models in elastodynamics [2,38]. Section 2 and Section 3 introduce preliminaries and discuss a prototype one-dimensional boundary value problem (BVP) with a solution that exhibits both slowly-varying and highly-oscillatory components. Section 4 gives the general XdG approach for these problems and Section 5 describes a specific XdG implementation, the Babuska-Zlamal method. Section 6 provides convergence and error results for the proposed method and Section 7 provides computational error results for the dG method and the XdG method for a number of example problems. We discuss conclusions and future directions in Section 8.

This paper is based on the thesis of the third author [39], written under the guidance of Professor Donald French and Benjamin Vaughan, Jr.

ELLIPTIC PROBLEM

We will consider the following prototype elliptic boundary value problem (BVP):

Find $U = U(x)$, such that

$$\begin{aligned} -U'' + cU &= f \ \ on \ \ \Omega = (0,\pi), \\ U'(0) &= U'(\pi) = 0, \end{aligned} \tag{1}$$

with $0 < c_0 \le c \le c\_1$. Here, c_0. and c_1. are constants and we assume that the functions $f(x)$, $c(x)$ and $U(x)$ are smooth functions. We chose this elliptic problem for its simplicity and we expect that the following analysis could be extended to more general elliptic problems in higher dimensions.

We specifically assume that the solution to this elliptic BVP, $U(x)$ belongs to a class of solutions that contain both slowly-varying and highly-oscillatory components. Hence, we require that the functions $f(x)$ and $c(x)$ are such that the solution has the general form:

$$\mathrm{U(x)} = \mathrm{S(x)} + \sum_{j=0}^{M} \Lambda_j(x)\cos\left(\omega_j x\right), \tag{2}$$

where $S(x)$ and $\Lambda_j(x)$ for $J = 1, \ldots, M$ are smooth in the sense that they have many derivatives, all of which have norms that are moderately sized and $0 < \omega_1 \le \omega_2 \le \ldots \omega_M$ are large numbers.

We further assume that the band $\omega_M - \omega_1$ is relatively small.

SOBOLEV SPACE NOTATION AND APPROXIMATION PRELIMINARIES

We use the following inverse inequality for functions $\chi \in P_q\left(\tau_j\right)$; there exists $C > 0$ which is independent of h so that

$$\left\|\chi\right\|_{\ell,\mathrm{p},\tau_j} \le Ch^{m-\ell+\frac{1}{p}-\frac{1}{r}} \left\|\chi\right\|_{m,\mathrm{r},\tau_j}, \tag{3}$$

for $m \le \ell$, $1 \le p \le \infty$, and $1 \le r \le \infty$. We also assume there is an interpolation operator

$\pi_h : W^{q+1,p}\left(I_j\right) \to P\left(I_j\right)$ (Theorem 4.4.4, [50]) with the following estimate

$$\left\|\left(I-\pi_h\right)v\right\|_{\ell,p,I_j} \le Ch^{r-\ell}\left\|v\right\|_{r,p,I_j} \quad \left(0 \le \ell \le r \le q+1\right), \tag{4}$$

and $\pi_h\left(\xi\right) = \xi$ for $\xi \in P_q\left(I_j\right)$. Moreover, if $v \in C\left(\bar{\Omega}\right)$ then $\pi_h v$ is continuous on $\bar{\Omega}$ as well. The *arithmetic-geometric mean inequality* states that for scalars a and b, $|ab| \le \delta a^2 + C_\delta b^2$, where $C_\delta = (4\delta)^{-1}$ and $\delta > 0$.

We now directly approximate the form (2) using interpolation in the space $E_h^q(\Omega)$; let

$$U_A(x) = \pi_h S(x) + \sum_{\ell=n_o}^{n_t} \begin{bmatrix} \left(\pi_h\alpha_\ell\right)(x)\cos(\ell x) \\ +\left(\pi_h\beta_\ell\right)(x)\sin(\ell x) \end{bmatrix}.$$

Note that $U_A \in E_h^q(\Omega)$ and thus

$$U(x) - U_A(x) = \left(I-\pi_h\right)S(x) + \sum_{\ell=n_o}^{n_t} \begin{bmatrix} \left(1-\pi_h\right)\alpha_\ell(x)\cos\left(n_\ell x\right) \\ +\left(1-\pi_h\right)\beta_\ell(x)\sin\left(n_\ell x\right) \end{bmatrix}.$$

So using (32), there is constant C, independent of h and the ω_ℓ, so

$$\left\|U - U_A\right\|_{m,q,\tau_j} \le Ch^{q+1-m}\omega_L^m \quad 0 \le m \le r \le q+1. \tag{5}$$

Also, since U is continuous, it follows that U_A is as well.

EXTENDED DISCONTINUOUS GALERKIN METHOD FOR HIGHLY OSCILLATORY PROBLEMS

The one-dimensional version of our XdG scheme will use the $N + 1$ nodes, $0 = x_0 < x_1 < \ldots < x_N = 1$, that define N individual elements $\tau_j = [x_{j-1}, x_j]$ with element lengths $h_j = x_j - x_{j-1}$ for $j = 1,2,\ldots, N$. More precisely, we assume that there exists a family of meshes J_h that depends on the element length h. We assume the mesh is quasi-uniform so that $h_j \approx h = N^{-1}$. We will use the approximation space $D_h^q(\Omega)$ that contains functions which are discontinuous piecewise polynomials of degree at most q over the family J_h and are discontinuous across the element boundaries. We let $P_r(S)$ denote the set of polynomials of degree r restricted to an interval S.

To approximate the highly-oscillatory parts of the solution, we enrich the standard dG approximation space with a range of Fourier series components. The "enriched" space, $E_h^q(\Omega)$ consists of functions of the form

$$\mathscr{y}(x) = S(x) + \sum_{j=1}^{L}\left[a_j(x)\cos\left(n_j x\right) + b_j(x)\sin\left(n_j x\right)\right] \tag{6}$$

where $s, a_j, b_j \in D_h^q(\Omega)$ and $n_j \in \mathbb{R}$ for $j = 1,\ldots, L$. Note that if we know the frequencies $\omega_1, \ldots, \omega_M$ *a priori*, we can let $L = M$ and $n_j = \omega_j$ for $j = 1,\ldots, M$. Otherwise, we note that

$$\begin{aligned} \Lambda_j(x)\cos\left(\omega_j x\right) &= \Lambda_j\cos\left(n_j x + \left(\omega_j - n_j\right)x\right) \\ &= \Lambda_j(x)\cos\left(\Delta\omega_{j,k}x\right)\cos\left(n_k x\right) \\ &\quad - \Lambda_j(x)\sin\left(\Delta\omega_{j,k}x\right)\sin\left(n_k x\right) \end{aligned} \tag{7}$$

where $\Delta\omega_{j,k} = \omega_j - n_k$ for a given j and k. If $\Delta\omega_{j,k}$ is small, then the functions

$$a_j(x) = \Lambda_j(x)\cos\left(\Delta\omega_{j,k}x\right)$$
$$b_j(x) = -\Lambda_j(x)\sin\left(\Delta\omega_{j,k}x\right) \quad (8)$$

are smooth since their frequencies are small. Hence, they can be well approximated by functions in $D_h^q(\Omega)$. This allows us to not know the exact frequencies *a priori* if we have a good approximation of their values as well as not requiring us to include all large frequencies if they exist subsets that have a small bandwidth, i.e., $|\omega_i - \omega_j|$ small for the some $i, j \in \{1,2\ldots,M\}$ with $i \neq j$.

BABUSKA-ZLAMAL XDG METHOD

We use the Babuska-Zlamal (BZ) method \cite{BZ} as a simple starting point for our approach since the analysis is more straightforward but the BZ method's use of a "super penalty" for stabilization can lead to ill-conditioning, which limits its practical use.

The BZ-XdG method for the problem (1) is defined as: Find $u \in E_h^q(\Omega)$ such that

$$\mathrm{B}(\mathrm{u},\phi) + \mathrm{h}^{-\theta}\sum_{j=1}^{N-1}[u]\left(x_j\right)[\phi]\left(x_j\right) = (f,\phi) \;\; \forall \phi \in E_h^q(\Omega), \quad (9)$$

where $\theta > 0$ will be determined later. The bilinear operator $B(\cdot,\cdot)$ is given by

$$\mathrm{B}(\mathrm{u},\phi) := \sum_{j=1}^{N}\int_{\tau_j} u'\phi' dx + \int_\Omega c(x)u\phi\, dx, \quad (10)$$

here (f,ϕ) is the inner product,

$$(\mathrm{f},\phi) = \int_\Omega f\phi dx \quad (11)$$

and [u] *is the jump operator,*

$$[u]\left(x_j\right) = \lim_{x\to x_j^+} u(x) - \lim_{x\to x_j^-} u(x). \quad (12)$$

Note that letting $u = \phi$ leads to a stability estimate from which existence and uniqueness can be proved. Further, recall that this method is inconsistent in the sense that the true solution U of (1) does not satisfy the variational form of the differential equation in (6). This is because an inter-element term arising from the integration-by-parts step is left out in BZ schemes. For the original BVP, (1) we have, after multiplying by $\phi \in E_h^q(\Omega)$ and integrating-by-parts,

$$B(U,\phi) + \sum_{j=1}^{N-1} U'\left(x_j\right)[\phi]\left(x_j\right) = (f,\phi), \quad (13)$$

ERROR ANALYSIS

We begin by denoting that u is the solution to the BZ-XdG problem, (6), U is the exact solution to elliptic equation, (1), and $U_A = \pi_h U$ is the interpolation of U using the enriched space $E_h^q(\Omega)$, (3).

We use the error splitting $e = u - U = \eta + (U_A - U)$ where $\eta = u - U_A$. Then, for $\phi \in E_h^q(\Omega)$

$$\begin{aligned} B(U_A,\phi) &= B(U_A - U,\phi) + B(U,\phi) \\ &= B(U_A - U,\phi) + \left[(f,\phi) - \sum_{j=1}^{N-1} U'\left(x_j\right)[\phi]\left(x_j\right)\right] \end{aligned} \quad (14)$$

where we used (10). Now, subtracting (11) from (6), we obtain

$$\begin{aligned} B(\eta,\phi) + h^{-\theta}\sum_{j=1}^{N-1}[u]\left(x_j\right)[\phi]\left(x_j\right) &= -B(U_A - U,\phi) \\ &\quad + \sum_{j=1}^{N-1} U'\left(x_j\right)[\phi]\left(x_j\right). \end{aligned} \quad (15)$$

Taking $\phi = \eta$ and noting that U_A is continuous so that $[U_A(x_j) = 0$ for $j = 1, \ldots, N$, we have

$$\begin{aligned} B(\eta,\eta) + h^{-\theta}\sum_{j=1}^{N-1}[\eta]\left(x_j\right)^2 &= -B(U_A - U,\eta) \\ &\quad + \sum_{j=1}^{N-1} U'\left(x_j\right)[\eta]\left(x_j\right) =: T_1 + T_2. \end{aligned} \quad (16)$$

We now estimate the second term using the Cauchy-Schwarz inequality and the Arithmetic-Geometric mean as follows:

$$|T_2| \le \left(h^\theta\sum_{j=1}^{N-1}\left|U'\left(x_j\right)\right|^2\right)^{\frac{1}{2}}\left(h^{-\theta}\sum_{j=1}^{N-1}\left|[\eta]\left(x_j\right)\right|^2\right)^{\frac{1}{2}},$$

or, for some $\delta > 0$,

$$|T_2| \le C_\delta h^{-\theta}\sum_{j=1}^{N-1}\left|U'\left(x_j\right)\right|^2 + \delta h^{-\theta}\sum_{j=1}^{N-1}\left|[\eta]\left(x_j\right)\right|^2.$$

If we let $\delta = 1/2$ then there exists $C > 0$ so

$$B(\eta,\eta) + h^{-\theta}\sum_{j=1}^{N-1}[\eta]\left(x_j\right)^2 \le C\begin{pmatrix}\left|B(U_A - U, U - U_A)\right| \\ +h^\theta\sum_{j=1}^{N-1}\left|U'\left(x_j\right)\right|^2\end{pmatrix}.$$

So, now, there is a $C > 0$ independent of h and ω_L such that

$$\|\eta\|_{1,h}^2 + h^{-\theta}\sum_{j=1}^{N-1}[\eta](x_j)^2 \le C\left(\|U-U_A\|_{1,2,\Omega}^2 + h^{\theta}\sum_{j=1}^{N-1}\left|U'(x_j)\right|^2\right)$$
$$\le C\left(h^{2q} + Nh^{\theta}\right)\omega_L^2.$$

Since $N = \frac{\pi}{h}$, it is natural to choose $\theta = 2q + 1$ and conclude

$$\|\eta\|_{1,h} \le Ch^q\omega_L.$$

Combining this with (5) and the triangle inequality, we have our main estimate:

$$\|u-U\|_{1,h} \le Ch^q\omega_L. \tag{17}$$

COMPUTATIONAL RESULTS

To evaluate the practical performance of the proposed method, we provide the results of various numerical computations for the model elliptic problem, (1), as well as for an alternate BVP that was not analyzed, the Helmholtz equation.

For the elliptic problem, we solve

$$-U'' + c(x)U = f(x) \text{ in } 0 < x < \pi \tag{18}$$

with the boundary conditions $U(0) = U(\pi) = 0$. For the functions $c(x) = \omega^2 + 1$ and $f(x) = -2\omega\cos(\omega x)$, the solution is

$$U(x) = \frac{e^x}{\omega^2+1}\left(\sin(\omega x) - \omega\cos(\omega x)\right).$$

For this problem, our approximation spaces is constructed from quadratics ($q = 2$) with one set of trigonometric function, $L = 1$, with $n_1 \approx \omega$ so each element consists of $m = 3$ shape functions for the unenriched dG space and $m = 9$ shape functions (three unenriched and six enriched) for the XdG space within each element. The domain is discretized into N elements of uniform length, $h_n = h = \frac{\pi}{N}$, which generates a total of $9N$ degrees of freedom (DOF) for the XdG system and $3N$ DOF for the dG system.

The mass and stiffness matrix integrals were all done on a reference element $\hat{\tau} = [-1, 1]$ where we used $n_{QP} = 10$ Gauss-Lobatto point numerical integration. The transformation from $[x_n, x_{n+1}] \to [-1, 1]$ was done by function $X(s) = \frac{h(s+1)}{2} + x_n$ and we had, if ϕ_ℓ and $\widehat{\phi_\ell}$ are basis and shape functions, respectively, then

$$\int_{x_n}^{x_{n+1}} \phi_i'(x)\phi_j'(x)\,dx = \frac{2}{h}\int_{-1}^{1}\widehat{\phi_i'(s)}\widehat{\phi_j'(s)}\,ds$$
$$\int_{x_n}^{x_{n+1}} c(x)\phi_i(x)\phi_j(x)\,dx = \frac{h}{2}\int_{-1}^{1} c(X(s))\widehat{\phi_i(s)}\widehat{\phi_j(s)}ds$$
$$\int_{x_n}^{x_{n+1}} f(x)\phi_i(x)\,dx = \frac{h}{2}\int_{-1}^{1} f(X(s))\widehat{\phi_i(s)}\,ds$$

To implement the stabilization terms, we note that if

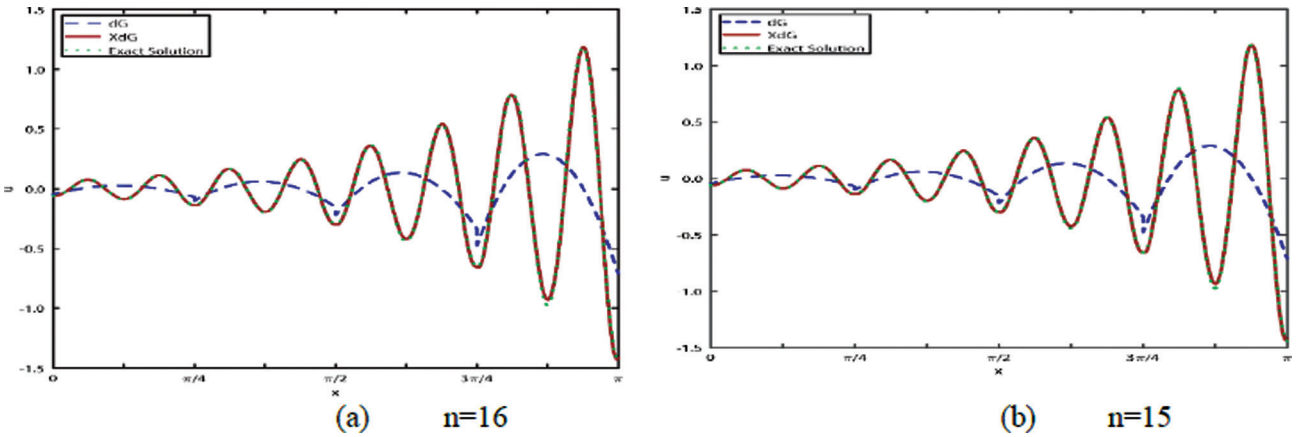

Figure 1. Numerical solution of (18) for a single oscillatory mode $\omega = 16$, using the dG (dashed blue curve) and XdG (solid red curve) approximations with $N = 4$ elements. The exact solution is shown as the green dotted curve, which closely coincides with the XdG solution. The XdG approximation shown in 1a uses the exact mode ($n = \omega = 16$) and 1b uses an approximation of the exact mode ($n_1 = 15$). We can see that even with only four elements, the XdG approximations are both quite accurate while the dG approximation is unresolved, as expected. The use of an approximate value of ω instead does not negatively effect the error in the approximation. The maximum absolute error for the dG approximation in both figures is 1.2×10^6 and for the XdG approximations is 4.0×10^{-2} for $n = 15$ and 4.6×10^{-2} for $n = \omega = 16$.

$$\mathrm{u}(\mathrm{x}) = \sum_{j=1}^{Nm} c_j \phi_j(x),$$

then

$$\sum_{k=1}^{N-1} [u](x_k)[\phi_i](x_k) = \sum_{j=1}^{Nm} c_j \left(\sum_{k=1}^{N-1} [\phi_j](x_k)[\phi_i](x_k) \right).$$

We define

$$J_{ik}^{+} = \phi_i\left(x_k^{+}\right) \text{ and } J_{ik} = J_{ik}^{+} - J_{ik}^{-}$$

where $\mathrm{J} \in \mathbb{R}^{Nm \times N-1}$ then

$$\sum_{k=1}^{N-1} [u](x_k)[\phi_i](x_k) = \mathrm{J}\mathrm{J}^T \mathrm{c},$$

where the components of the vector c are $c_i = c(x_i)$.

The numerical solution of (18) is shown in Figure 1 for the dG approximation (dashed blue curve) and the XdG approximation (solid red curve) with a single mode ω = 16 using four elements (N = 4). The exact solution is represented by the dotted green curve. For XdG method, we computed the solution with $n = \omega = 16$ (Figure 1a as well as a mode close to the exact mode, n = 15 Figure 1b).

We can see that, as expected, the XdG approximation captures the oscillatory behavior quite well even with using an approximation of ω (n_1 = 15) while the dG approximation is not able to resolve the oscillations for the given discretization.

Figure 2 show the convergence results for the dG and XdG methods.

The observed rate of convergence for both XdG approximations exceed the theoretical rate of convergence with an absolute error going below 10^{-6} for less than 20 elements. For the dG approximation, the observed rate of convergence is close to the theoretical estimate (p = 3) for quadratic elements.

For small values of ω, the practical benefit of the XdG approach is lessened since it does not require many elements to resolve the oscillations. Once a sufficient number of elements are used, the dG method does sufficiently good job of approximating the solution but for larger values of ω, a significant number of elements are needed to resolve the highly-oscillatory behavior before convergence is observed.

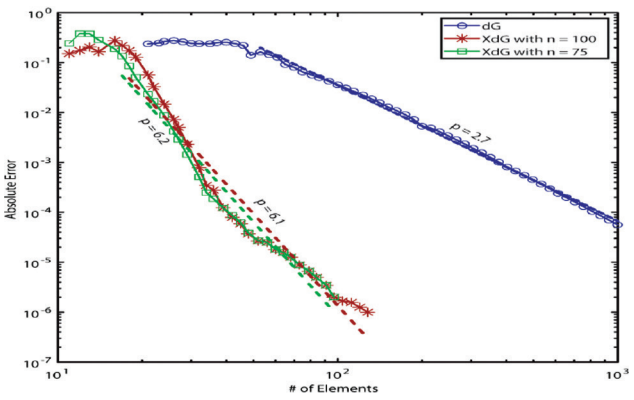

Figure 3.

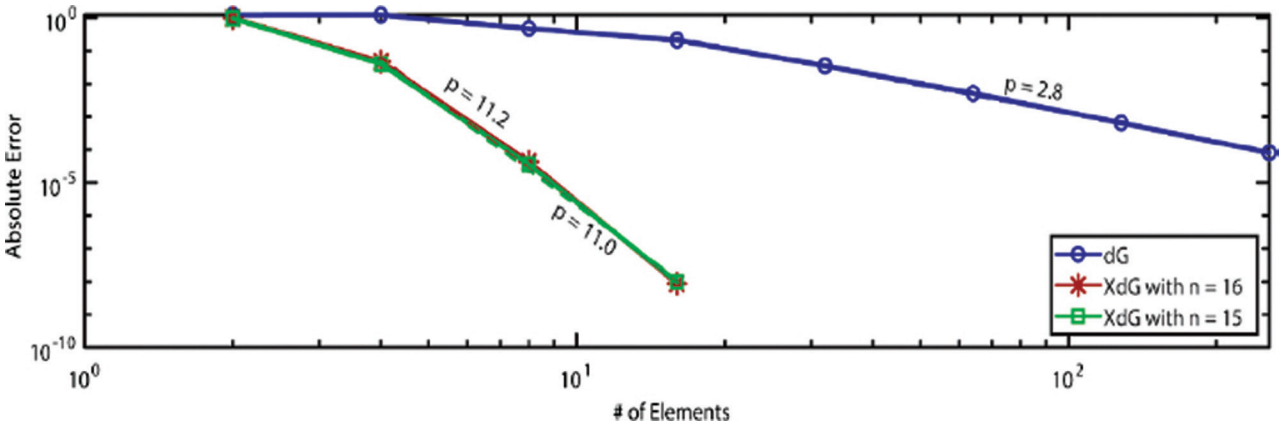

Figure 2. Log-log plot of the absolute error for the dG and XdG approximations versus the number of elements for ω = 16. We can see that both XdG approximations converge much more rapidly than the dG approximation. The p values indicate rate of convergence from linear least-squares fits of the log-log error. For the dG approximation, the observed rate of convergence is close to the theoretical order of convergence since we use quadratic elements. For the XdG approximations, the observed rate of convergence is significantly higher and similar for both $n = \omega$ = 16 and n = 15.

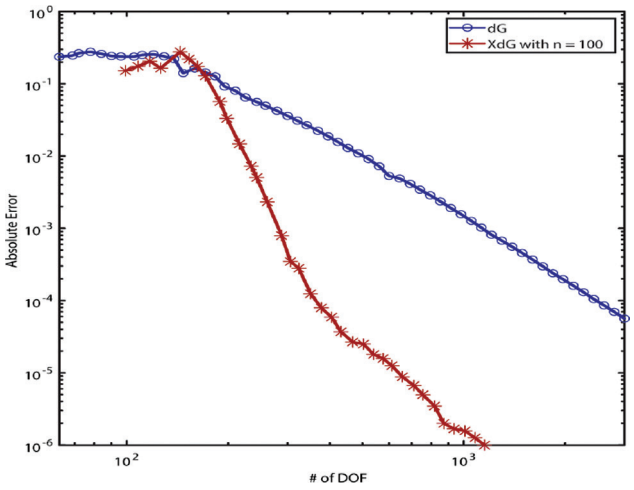

Figure 4. DOF v.s. Error.

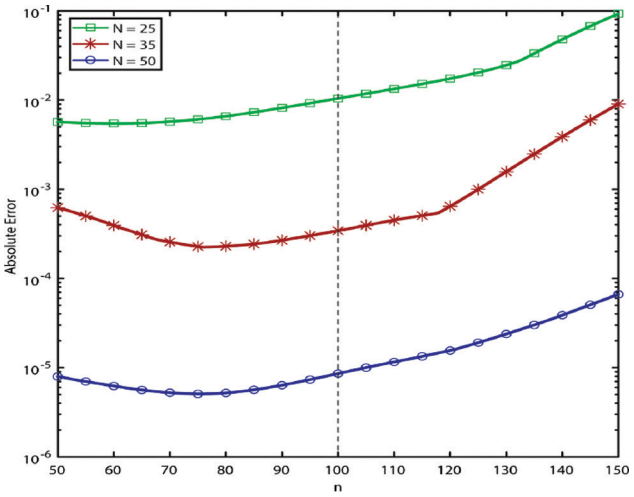

Figure 5.

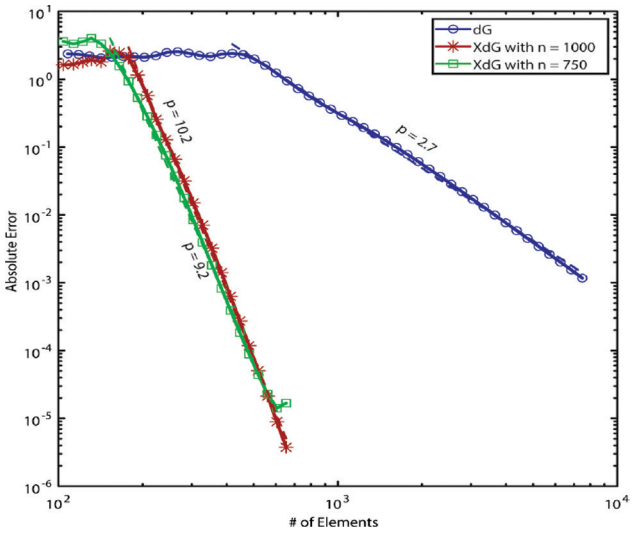

Figure 6.

In this regime, the XdG approach can lead to a significant reduction in the number elements required.

Figure 3 shows the convergence results for the dG and XdG methods when solving the elliptic benchmark problem for $\omega = 100$.

We can see that the XdG method resolves the highly-oscillatory behavior for an order of magnitude fewer elements than required by the dG method. We additionally see a higher rate of convergence using the XdG method versus dG. These are both true if we choose $n = \omega$ or $n = 75$, which is the same order of magnitude as ω but off by 25%. The XdG method still resolves the oscillations as well as when $n = \omega$ and converges at the same rate. This suggests that the exact frequency of highly-oscillatory components does not need to be know a priori but can be estimated to retain the benefits of the XdG method.

Since the enrichments add additional DOFs to the system (nine DOFs per element for XdG versus three DOFs per element for the dG), we compare the convergence both methods in terms of DOFs, as shown in Figure 4.

We see that approximately the same number of DOFs are required before convergence is observed but the rate of convergence is significantly higher for the XdG method, with the absolute error approximately 10^{-6} for 1000 DOFs (approximately 100 elements) vs 10^{-2} when using the dG method.

Since we still observe convergence when $n \neq \omega$, we computed the absolute error as the value of n is varied. Figure 5 shows that the absolute error is roughly the same order of magnitude when n is near ω and is increasing as n increases through ω.

This suggests that if ω is not know a priori, underestimating ω could reduce the error. Additionally, choosing $n = \omega$ might not be the optimal choice to reduce the error.

In Figure 6, we study the convergence for an even higher frequency, $\omega = 1000$. Again the XdG method starts converging an order of magnitude sooner than the dG method and converges at a higher rate.

The XdG methods requires 200 elements before convergence begins but, since we included the exact mode in our approximation, one might suspect that the highly-oscillatory component of the solution would be resolved sooner and convergence would begin for a smaller number of elements. This is not observed here due to our choice of the BZ method. This approach is not a consistent numerical method and would not expect to obtain the exact solution, which reduces the effectiveness of this version of the XdG method. Using an improved version of dG as a base

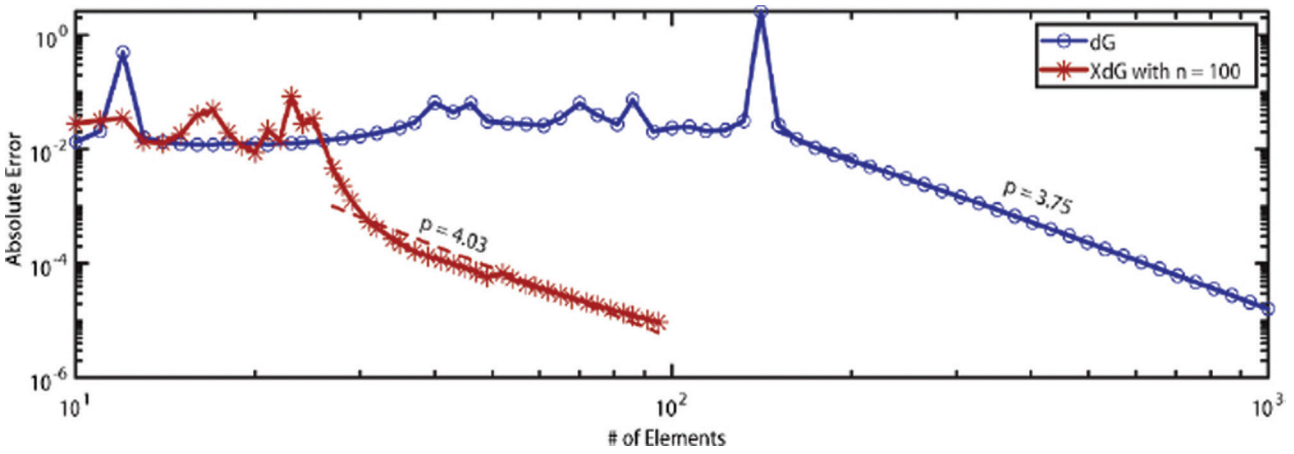

Figure 7.

method for the XdG approach, such as symmetric interior penalty discontinuous Galerkin (SIPG) method, could reduce the minimum number of elements before convergence is observed as well as improving the conditioning of the resulting linear systems.

Although our theory does not extend to the Helmholtz equations, we measured the convergence of the XdG method applied to the benchmark Helmholtz problem:

$$-U'' + \omega^2 U = \omega^2 x \text{ for } 0 < x < \pi \qquad (19)$$

with the boundary conditions $U'(0) - u'(\pi) = 0$ and $\omega \in \mathbb{R}^+$. We choose $\omega \notin Z$ to prevent non-uniqueness. The solution of (19) is

$$U(x) = x + \frac{1}{\omega \sin(\omega x)}\left[\cos(\omega x) + \cos(\omega(\pi - x))\right].$$

Figure 7 shows the convergence results for the XdG and dG methods for our benchmark Helmholtz problem, (19), with ω = 100.3. For the XdG solution, we used the nearest integer value near ω in our approximation, n = 100. As before, we see that the XdG method begins converging for an order of magnitude less elements than is required for the dG method. The rate of convergence is comparable between the two methods.

CONCLUSIONS AND FUTURE DIRECTIONS

In this paper, we introduced an extended discontinuous Galerkin finite element method for approximating highly-oscillatory solutions based on Babuska-Zlamal method. We were able to provide an a priori error estimate for a prototype elliptic problem. This error estimate is similar to standard dG error estimates except that it scales linearly with increasing frequency while the dG approximation scales as a polynomial of one degree higher than the order of approximation basis. This implies that the XdG approach requires fewer elements to reduce the error below a desired tolerance when compared with the dG method. Additionally, it would theoretically allow the use of higher-order element basis functions without increasing the number of elements to keep the approximation below a desired tolerance.

In addition to the theoretical error bounds, we performed numerical simulations on various benchmark problems over a range of frequencies. We see that the XdG method, even using the BZ approximation that has poor practical performance, is able to resolve the high-frequency oscillations using an order of magnitude less elements and often shows a faster rate of convergence when compared with the dG method.

While knowing the exact frequency in the solution would allow us to generate a function space that contains the solution, the XdG method does not require this frequency to be known a priori. If one has a reasonable close estimate of the frequency, the XdG method generates highly accurate solutions. This could be useful when approximating problems that have the spatial frequency vary in space and time within reasonably small range. Since the exact frequency would not be known a priori, the XdG method should still provide good results using a reasonable approximation of the frequency.

In addition to studying our benchmark elliptic problem, we also examined a benchmark Helmholtz problem. While our analysis is not directly applicable, numerical simulations show that the XdG approach is able to able to resolve high-frequency components with fewer elements when compared with the dG method. This suggests that solving problems with high-frequency components to the solution

within a larger domain could be more computationally feasible due to the reduced number of elements required to resolve the solution.

The method described and analyzed in this paper is very preliminary and has a number of theoretical and practical limitations. The analysis is only applicable to the benchmark elliptic problem but we believe that it can be extended to other problems with highly-oscillatory solution such as the Helmoltz equation as well as time dependent problems such as the wave equation or problems with frequencies that vary in time or space. Additionally, the XdG method is an extension of the dG method, which is an extension of the continuous finite element method, so it is straight forward to adapt to nonlinear problems. These different mathematical problems have applications in a wide range of area such as simulating high-intensity focused ultrasound (HIFU) therapy [3] or coupled multiscale continuum/molecular dynamics models.

The choice of using the BZ method in deriving our current XdG approach was done out of simplicity in both the implementation and the analysis. An improvement that will greatly increase the usability of the XdG approach would be to switch to an alternative dG foundation such as the symmetric interior penalty Galerkin (SIPG) method [19]. This method is consistent and is better conditioned than the BZ method. We plan to extend our analysis and our implementation to use SIPG as an alternative approach.

AUTHORSHIP CONTRIBUTIONS

Authors equally contributed to this work.

DATA AVAILABILITY STATEMENT

The authors confirm that the data that supports the findings of this study are available within the article. Raw data that support the finding of this study are available from the corresponding author, upon reasonable request.

CONFLICT OF INTEREST

The author declared no potential conflicts of interest with respect to the research, authorship, and/or publication of this article.

ETHICS

There are no ethical issues with the publication of this manuscript.

REFERENCES

[1] Gracie R, Wang H, Belytschko T. Blending in the extended finite element method bydiscontinuous Galerkin and assumed strain methods. Int J Num Meth Eng 2008;74:1645-1669. [CrossRef]

[2] Yang Y, Chirputkar S, Albert DN, Eason Spottswood T, Qian D. Enriched space-time finite element method: a new paradigm for multiscaling from elastodynamics to molecular dynamics (Preprint).

[3] Huttunen JMJ, Huttunen T, Malinen M, Kaipio JP. Determination of heterogeneousthermal parameters using ultrasound induced heating and MR thermal mapping. Phys Med Biol 2006;51:1011-1032. [CrossRef]

[4] Petzold L.R, Jay L. O, Yen J. Numerical solution of highly oscillatory ordinary differentialequations. Acta Numerica 1997;6:437-483. [CrossRef]

[5] Garrido P.L, Goldstein S, Lukkarinen J, Tumulka R. Paradoxial reflection in quantummechanics (Preprint), 2008. [CrossRef]

[6] Ihlenburg F, Babuška I. Finite element solution of the Helmholtz equation with high wavenumber. Part I: The h-version of the FEM. Comp Math Appl 1995;30:9-37. [CrossRef]

[7] Ihlenburg F, Babuška I. Solution of Helmholtz problems by knowledge-based FEM. Comp Assisted Mech Eng Sci 1997;4:397-415.

[8] Thompson LL. A review of finite-element methods for time-harmonic acoustics. J Acoust Soc Am 2006;119:1315–1330. [CrossRef]

[9] Babuška I, Melenk JM. The partition of unity method. Int J Num Meth Eng 1997; 40: 727-758. [CrossRef]

[10] Monk P, Wang D.-Q. A least-squars method for the Helmholtz equation. Comput Methods Appl Mech Eng 1999;175:121-136. [CrossRef]

[11] Cessenat O, Després B. Application of the ultraweak variational formulation of ellipticPDEs to the 2-dimensional Helmholtz problem. SIAM J Numer Anal 1998;35:255–299. [CrossRef]

[12] Cessenat O, Despřes B. Using plane waves as base functions for solving time harmonicequations with the Ultra Weak Variational Formulation. J Comput Acoustics 2003;11:227–238. [CrossRef]

[13] Huttunen T, Kaipio J, Monk P. The perfectly matched layer for the ultra weak variationalformulation of the 3D Helmholtz equation. Int J Numer Meth Eng 2004;61:1072–1092. [CrossRef]

[14] Luostari T, Huttunen T, Monk P. Improvements for the ultraweak variational formulation. Int J Numer Methods Eng 2013;94:598–624. [CrossRef]

[15] Huttunen T, Gamallo P, Astley RJ. Comparison of two wave element methods for the Helmholtz problem. Commun Numer Methods Eng 2009;25:35–52. [CrossRef]

[16] Wang D, Tezaur R, Toivanen J, Farhat C. Overview of the discontinuous enrichmentmethod, the ultraweak variational formulation, and the partition of unity method for acous-tic scattering in the medium

frequency regime and performance comparisons. Int J Numer Methods Eng 2012;89:403-417. [CrossRef]
[17] Reed WH, Hill TR. Triangular mesh methods for the neutron transport equation. Tech Report LA-UR-73-479, Los Alamos Scientific Laboratory, 1973.
[18] Hesthaven JS, Warburton T. Nodal Discontinuous Galerkin Methods: Algorithms, Analysis, and Applications. Springer Texts in Applied Mathematics 54. New York: Springer Verlag, 2008. [CrossRef]
[19] Rivière B. Discontinuous Galerkin methods for solving elliptic and parabolic equations, 35, Front Appl Math Philadelphia: SIAM, 2008. [CrossRef]
[20] Strouboulis T, Babuška I, Copps K. The design and analysis of the generalized finite element method. Comput Methods Appl Mech Eng 2000;181:43-69. [CrossRef]
[21] Strouboulis T, Copps K, Babuška I. The generalized finite element method: an exampleof its implementation and illustration of its performance. Int J Numer Methods Eng 2000;47:1401-1417. [CrossRef]
[22] Belytschko T, Black T. Elastic crack growth in finite elements with minimal remeshing. Int J Numer Meth Eng 1999;45:601-620. [CrossRef]
[23] Sukumar N, Moes N, Moran B, Belytschko T. Extended finite element method for three dimensional crack modelling,Int. J. Numer Methods Eng 2000;48:1549–1570. [CrossRef]
[24] Strouboulis T, Copps K, Babuška I. The generalized finite element method. Comput Methods Appl Mech Eng 2001;190:4081-4193. [CrossRef]
[25] Strouboulis T, Zhang L, Babuška I. Generalized finite element method using mesh-based handbooks: application to problems in domains with many voids. Comput Methods Appl Mech Eng 2003:192:3109-3161. [CrossRef]
[26] Strouboulis T, Babuška I, Hidajat R. The generalized finite element method for Helmholtz equation: Theory, computation, and open problems. Comput Methods Appl Mech Eng 2006;195:4711-4731. [CrossRef]
[27] Strouboulis T, Hidajat R, Babuška I. The generalized finite element method for Helmholtz equation. Part II: Effect of choice of handbook functions, error due to absorbing boundary conditions and its assessment. Comput Methods Appl Mech Eng 2008;197:364-380. [CrossRef]
[28] Merle R, Dolbow J. Solving thermal and phase change problem with the eXtended finite element method. Comput Mech 2002;28:339-350. [CrossRef]
[29] Smith BG, Vaughan BL, Chopp DL. The extended finite element method for boundary layer problems in biofilm growth. Comm App Math Comp Sci 2007;2:35-56. [CrossRef]
[30] Chessa J, Belytschko T. An extended finite element method for two-phase fluids. J Appl Mech 2003;70:10-17. [CrossRef]
[31] Karihaloo B, Xiao Q. Modelling of stationary and growing cracks in FE framework without remeshing: a state-of-the-art review. Comput Struct 2003;81:119–129. [CrossRef]
[32] Abdelaziz Y, Hamouine A. A survey of the extended finite element. Comput Struct 2008;86:1141–1151.
[33] Toprakseven Ş. A space-time discontinuous Galerkin method for linear hyperbolic PDE's with high frequencies. Commun Fac Sci Univ Ank Ser A1 Math Stat 2020;69:213-231. [CrossRef]
[34] Sukumar N, Chopp D, Moes N, Belytschko T. Modeling of holes and inclusions by level sets in the extended finite element method. Comput Methods Appl Mech Eng 2001;190:6183–6200. [CrossRef]
[35] Legay A, Wang H, Belytschko T. Strong and weak arbitrary discontinuities in spectral finite elements. Int J Numer Methods Eng 2005;64:991–1008. [CrossRef]
[36] Gracie R, Wang H, Belytschko T. Blending in the extended finite element method by discontinuous Galerkin and assumed strain methods. Int J Numer Methods Engr 2008;74:1645-1669. [CrossRef]
[37] Shen Y, Lew A. Stability and convergence proofs for a discontinuous-Galerkin-based extended finite element method for fracture mechanics. Comput Methods Appl Mech Eng 2010;199:2360-2382. [CrossRef]
[38] Chirputkar S.U, Qian D. Coupled atomistic/continuum simulation based on an extended space-time finite element method. Comput Model Eng Sci 2008;850:1-18.
[39] Toprakseven Ş. Error Analysis of Extended Discontinuous Galerkin (XdG) Method. Dissertation Thesis. Ohio: University of Cincinnati, 2014.
[40] Brenne SC, Scott LR. The Mathematical Theory of Finite Element Methods. Berlin: Springer-Verlag, 1994. [CrossRef]
[41] Babuška I, Zlamal M. Nonconforming elements in the finite element method with penalty. SIAM J Num Anal 1973;10:863-875. [CrossRef]